View metadata, citation and similar papers at core.ac.uk

brought to you by CORE

You have downloaded a document from
RE-BUŚ
repository of the University of Silesia in Katowice

Title: 57Fe Mossbauer spectroscopy of radiation damaged allanites

Author: Dariusz Malczewski, A. Grabias

Citation style: Malczewski Dariusz, Grabias A. (2008). 57Fe Mossbauer spectroscopy of radiation damaged allanites. "Acta Physica Polonica A" (Vol. 114, nr 6 (2008), s. 1683-1690).

Uznanie autorstwa - Użycie niekomercyjne - Bez utworów zależnych Polska - Licencja ta zezwala na rozpowszechnianie, przedstawianie i wykonywanie utworu jedynie w celach niekomercyjnych oraz pod warunkiem zachowania go w oryginalnej postaci (nie tworzenia utworów zależnych).

UNIWERSYTET ŚLĄSKI W KATOWICACH
Biblioteka Uniwersytetu Śląskiego
Ministerstwo Nauki i Szkolnictwa Wyższego

Proceedings of the Polish Mössbauer Community Meeting 2008

^{57}Fe Mössbauer Spectroscopy of Radiation Damaged Allanites

D. Malczewski[a] and A. Grabias[b]

[a]Faculty of Earth Sciences, University of Silesia
Będzińska 60, 41-200 Sosnowiec, Poland
[b]Institute of Electronic Materials Technology
Wólczyńska 133, 01-919 Warszawa, Poland

Metamict minerals contain radioactive elements that degrade the crystal structure of the minerals. The degradation occurs primarily through progressive overlapping recoil nuclei collision cascades from α-decays of ^{238}U, ^{232}Th, ^{235}U and their daughter products. We report the results of ^{57}Fe Mössbauer spectroscopy, gamma-ray spectrometry and microprobe analysis of three partially metamict allanites, $(Ca,Ce,REE)_2(Fe^{2+},Fe^{3+})(Al,Fe^{3+})_2O[Si_2O_7][SiO_4](OH)$ where REE stands for rare earth elements. The samples were collected in pegmatites from Reno, Nevada (USA), Franklin, New Jersey (USA) and Nya Bastnas Field (Sweden). The absorbed α-dose for these minerals was found to range from 5.8×10^{14} α-decay/mg for the allanite from Reno to 1.9×10^{15} α-decay/mg for the allanite from Franklin. The Mössbauer spectra show a decrease in the Fe^{2+} doublet intensity with increasing absorbed α-dose. We also observe an increase in the line widths of the Fe^{2+} and Fe^{3+} doublets with increasing absorbed α-dose.

PACS numbers: 33.45.+x, 61.82.Fd, 64.60.My, 76.80.+y

1. Introduction

Metamict minerals are a class of natural amorphous materials that were initially crystalline [1]. These minerals contain radioactive elements that degrade the crystal structure mainly by progressive overlapping recoil nuclei collision cascades from α-decays of ^{238}U, ^{232}Th, ^{235}U and their daughter products. Because of the natural occurrence of U and Th in these minerals, they serve as natural analogues for radiation effects in high level nuclear waste and are widely used in geochronology [2, 3]. Most silicates, such as zircon and gadolinite, become metamict after a cumulative α-dose of about 10^{16} α-decay/mg [3, 4]. The purpose of this work is to show that certain changes in hyperfine parameters of investigated metamict minerals are associated with the absorbed α-dose.

Allanite is a good example of a metamict mineral. Allanite belongs to the epidote group (a type of sorosilicate) [5] with monoclinic, $P21/m$ symmetry [6]. The epidote group can be represented by the ideal formula $A_2M_3Si_3O_{13}H$, where A indicates a large cation with high coordination number such as Ca, REE, U or Th, and the M sites are occupied by octahedrally coordinated trivalent and divalent cations such as Al^{3+}, Fe^{3+}, Fe^{2+}, Mn^{3+}, and Mg^{2+} [5]. The structure of allanite contains chains of edge-sharing MO_6 octahedra of two types, a single chain of M(2) octahedra completely occupied by Al^{3+} and a multiple chain composed of central M(1) (less distorted) and lateral M(3) (more distorted) octahedra. Iron ions are unequally distributed between the M(1) and M(3) sites. 83% of the total Fe is in the M(3) site.

2. Samples and experimental procedures

A sample of allanite from Reno, Washoe County, Nevada (ALL1) was collected from the Red Rock pegmatite bodies [7]. Crystal sections with dimensions of 0.3 to 2.5 cm were present in the rock matrix. The crystals were black and showed several good facies.

A sample of allanite from Nya Bastnas Field (ALL2) in central Sweden was collected from the Bastnas deposits containing mineral assemblages of Fe oxides, REE silicates, REE fluorocarbonates, sulfides of Cu, Mo, Bi, and others [8]. Brownish black, irregularly shaped crystal sections with dimensions from 0.5 to 2.5 cm were present in the massive copper and iron ore matrix of this allanite.

A sample of allanite from Franklin, Sussex County, New Jersey, was taken from the open cut pegmatite [9]. Black aggregates with dimensions from 0.2 to 2.5 cm were scattered in a pale greenish microcline matrix with minor quartz. All of the crystals in the allanites were carefully separated from their matrices. Basic characteristics of all the samples are given in Table I.

The concentrations of ^{232}Th, ^{238}U, and ^{235}U were calculated for each sample based on the gamma-ray activities of ^{228}Ac (^{232}Th), ^{226}Ra, ^{214}Pb, ^{214}Bi (^{238}U) and ^{235}U. Gamma-ray spectra were collected using an HPGe detector (32% efficiency with energy resolution of 0.8 keV at 122 keV) and analyzed using the Genie 2000 v.3 software package. Electron microprobe data were obtained using a JEOL JSM-6480 Scanning Electron Microscope operated at an accelerating voltage of 20 kV and analyzed using the EDS2006 software. The samples were ground into powder and prepared in the shape of a thin disc absorber. The Mössbauer transmission spectra were recorded at room temperature using a constant acceleration spectrometer, a multichannel analyzer with 512 channels and a linear arrangement of a ^{57}Co/Rh source (= 50 mCi) absorber and detector. All Mössbauer spectra were numerically analyzed by the fitting software MOS MOD and MEP and all doublets were considered as superpositions of an appropriate number of Lorentzian lines. X-ray powder diffraction (XRD) patterns were obtained using a PHILIPS X'Pert diffractometer in the $\Theta-\Theta$ system and Cu K_α radiation in scan mode with step size 0.02°.

TABLE I

Ages, chemical composition and calculated α-doses of allanite samples used.

	ALL1	ALL2	ALL3
Age [Ma]	145–200[a]	1863(13)[b]	986(4)[c]
O [wt.%]	29.61(41)	21.68(28)	20.09(33)
Si [wt.%]	21.44(16)	14.88(39)	17.13(16)
Al [wt.%]	4.21(12)	4.05(7)	4.15(8)
Ca [wt.%]	6.63(9)	5.53(8)	6.63(10)
Fe [wt.%]	11.90(14)	14.75(20)	13.43(21)
La [wt.%]	4.31(15)	7.55(21)	3.20(16)
Ce [wt.%]	9.88(23)	12.07(26)	9.13(28)
U [ppm]	89(4)	148(7)	49(2)
Th [ppm]	3917(31)	55(5)	2245(19)
Calculated total dose [α-decay/mg][d]	$5.8(8) \times 10^{14}$	$1.19(7) \times 10^{15}$	$1.95(2) \times 10^{15}$
Calculated dose from ^{232}Th [α-decay/mg]	$5.3(7) \times 10^{14}$	$8.5(18) \times 10^{13}$	$1.77(1) \times 10^{15}$

[a][7]. [b][8]. [c][9]. [d]Dose was calculated from the equation: $D = 8N_{238}(e^{t\lambda 238} - 1) + 7N_{235}(e^{t\lambda 235} - 1) + 6N_{232}(e^{t\lambda 232} - 1)$, where N_{238}, N_{235} and N_{232} are the present number of atoms of ^{238}U, ^{235}U and ^{232}Th per milligram, $\lambda_{238}, \lambda_{235}$ and λ_{232} are the decay constants of ^{238}U, ^{235}U and ^{232}Th, and t is the geologic age.

3. Results and discussion

The Mössbauer spectra of the allanite samples with the corresponding XRD patterns are shown in Fig. 1. The hyperfine parameters derived from the fitting procedure for each of the five samples are summarized in Table II.

3.1. Changes in hyperfine parameters of Fe^{2+} components as a function of α-dose

As expected, the Mössbauer spectra of allanites show doublets representing Fe^{2+} in the M(1) and M(3) octahedral sites. In all the spectra, Fe^{2+} in the M(1) site is represented by doublet no. 1, as labeled in Fig. 1 and Table II. In the spectra of ALL1 and ALL3, Fe^{2+} in the M(3) site is represented by doublets 2 and 3 (Fig. 1, Table II). The doublet no. 3 with lower isometr shift (IS) and quadrupole splitting (QS) values may be interpreted as representing the most distorted octahedra of the M(3) site, whereas doublet no. 2 represents the less distorted positions of Fe^{2+} in the M(3) site. The spectrum of sample ALL2 is characterized by the presence of one doublet, no. 2 (Fig. 1, Table II), representing Fe^{2+} in the M(3) site. The IS and QS values of this doublet are intermediate between the IS and QS values of doublets 2 and 3 in the ALL1 and ALL2 spectra. Similar results were presented in a paper dealing with the Mössbauer spectroscopy of epidote group minerals [10].

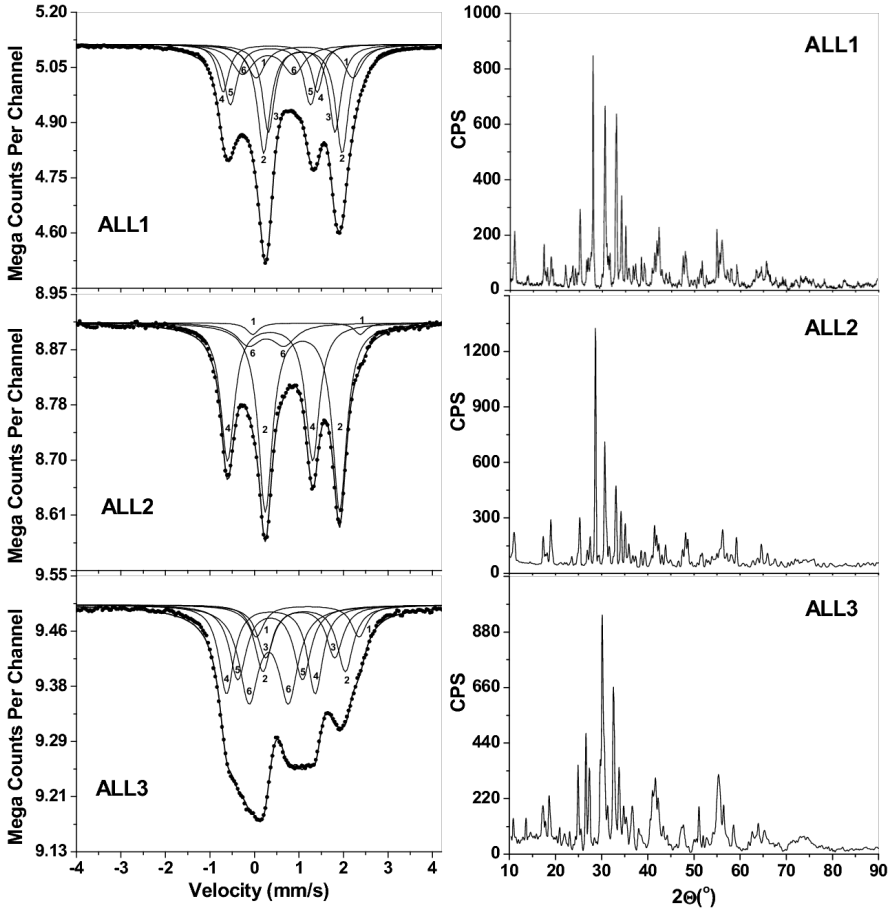

Fig. 1. (left hand plots) ^{57}Fe Mössbauer spectra at room temperature of allanite samples. Solid dots — experimental data; thick solid line — fitted curve; thin solid line — fitted doublets. (right hand plots) Corresponding XRD patterns.

Figure 2a shows the change in the relative contribution of Fe^{2+} ($\sum Fe^{2+}/\sum Fe$) as a function of the absorbed α-dose. The contribution of Fe^{2+} components decreases with absorbed total α-dose. This result is unexpected because the metamictization process is considered to be accompanied by the reduction of some of the Fe^{3+} to Fe^{2+} in the radiation damaged regions. Therefore, as α-decay damage increases, the amount of Fe^{2+} is expected to increase [11]. We are not certain how to explain the observed opposite effect in the allanites of this study. If α-dose is not a major controlling factor for the amount of Fe^{2+}, it seems probable that the initial ratio of Fe^{2+}/Fe^{3+} in the samples is of great importance. Further annealing experiments are needed to explain the observations.

Figure 2b shows weighted averages of the line widths of all Fe^{2+} components as a function of α-dose. As expected, the average line widths slightly increase

TABLE II

Hyperfine parameters from the ^{57}Fe Mössbauer spectra shown in Fig. 1 for investigated allanite samples. Isomer shift values (IS) are given relative to the α-Fe standard at room temperature.

Sample	Doublet no.	χ^2	IS [mm/s]	QS^a [mm/s]	Γ^b [mm/s]	Assignment (CN)^c	Intensity
ALL1		1.5					
	1		1.12(1)	2.17(4)	0.25(2)	Fe^{2+}(6) M1	0.12(1)
	2		1.09(1)	1.76(1)	0.17(1)	Fe^{2+}(6) M3	0.28(2)
	3		1.06(1)	1.49(2)	0.16(1)	Fe^{2+}(6) M3	0.21(1)
	4		0.35(1)	2.11(3)	0.16(1)	Fe^{3+}(6) M3	0.11(2)
	5		0.36(1)	1.80(3)	0.18(2)	Fe^{3+}(6) M3	0.16(2)
	6		0.31(1)	1.15(3)	0.28(2)	Fe^{3+}(6) M1	0.12(2)
ALL2		1.5					
	1		1.17(2)	2.42(4)	0.16(1)	Fe^{2+}(6) M1	0.030(3)
	2		1.08(1)	1.67(1)	0.19(1)	Fe^{2+}(6) M3	0.51(3)
	4		0.35(1)	1.91(1)	0.18(1)	Fe^{3+}(6) M3	0.36(2)
	6		0.28(2)	0.84(3)	0.29(2)	Fe^{3+}(6) M1	0.10(1)
ALL3		1.4					
	1		1.19(3)	2.31(3)	0.23(3)	Fe^{2+}(6) M1	0.10(2)
	2		1.09(1)	1.82(4)	0.21(3)	Fe^{2+}(6) M3	0.16(2)
	3		1.03(3)	1.52(2)	0.21(2)	Fe^{2+}(6) M3	0.10(1)
	4		0.36(1)	1.99(2)	0.21(1)	Fe^{3+}(6) M3	0.20(2)
	5		0.35(1)	1.45(2)	0.22(2)	Fe^{3+}(6) M3	0.18(2)
	6		0.32(1)	0.88(3)	0.26(2)	Fe^{3+}(6) M1	0.26(3)

^{a}Quadrupole splitting. ^{b}Line width. ^{c}Coordination number.

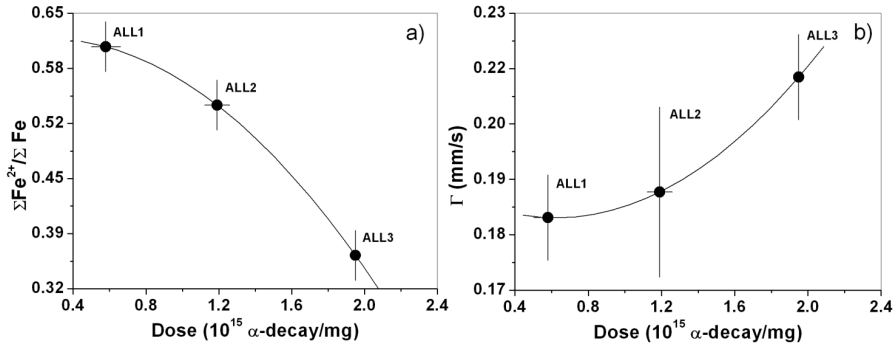

Fig. 2. (a) $\sum \mathrm{Fe}^{2+} / \sum \mathrm{Fe}$ vs. absorbed α-dose; the solid line represents polynomial fit: $(\sum \mathrm{Fe}^{2+} / \sum \mathrm{Fe}) = 0.615 + 0.042D - 0.089D^2$, correlation coefficient $r = -0.98$. (b) Average line widths of Fe^{2+} components versus absorbed α-dose; the solid line represents polynomial fit: $\Gamma = 0.189 - 0.023D + 0.089D^2$, correlation coefficient $r = 0.96$.

with absorbed α-dose. Figures 3a and b show weighted averages of quadrupole splittings for Fe^{2+} doublets versus total absorbed α-dose and versus absorbed α-dose from the ^{232}Th series, respectively. As seen in Fig. 3, plotting the quadrupole splittings as a function of the α-dose from ^{232}Th gives a better correlation than plotting as a function of total α-dose.

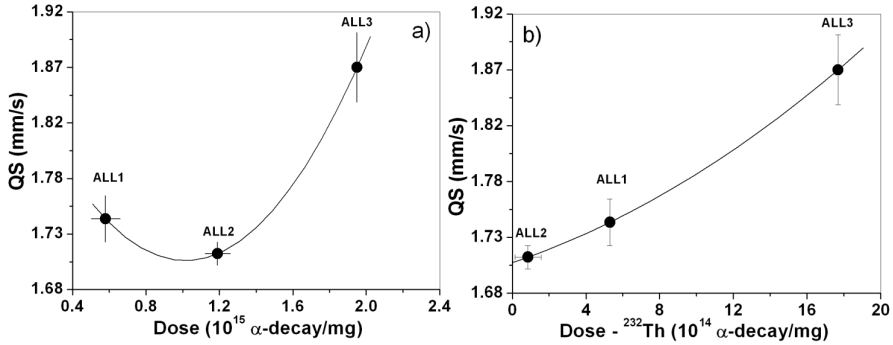

Fig. 3. Averages of quadrupole splittings of Fe^{2+} components versus: (a) absorbed total α-dose and (b) absorbed α-dose from the ^{232}Th series. The solid lines represent polynomial regressions: $QS = 1.90 - 0.386D + 0.19D^2$ and $QS = 1.706 + 0.005D_{Th} + 0.0002D_{Th}^2$. The correlation coefficients are $r = 0.80$ and 1, respectively.

The sample ALL1 is characterized by half the total α-dose absorbed by ALL2. On the other hand, from ^{232}Th decay, ALL1 has an α-dose six times higher than that of ALL2, as shown in Table I. The average energy of α particles from the ^{232}Th series is 6.14 MeV and the average energy of recoil nuclei is about 105 keV. These values are higher than for the ^{238}U series, where the average energy of α particles and of recoil nuclei are 5.34 MeV and 89 keV, respectively. The α-decays from the ^{232}Th series cause larger radiation damage than α-decays from ^{238}U. This may be why the experimental parameters for samples ALL1 and ALL2 are very similar despite the total α-dose for sample ALL2 being twice that of ALL1. Isomer shift values of Fe^{2+} components do not show noticeable changes. The average IS values range from 1.09(1) mm/s for samples ALL1 and ALL2 to 1.10(1) mm/s for ALL3.

3.2. Changes in hyperfine parameters of Fe^{3+} components as a function of dose

In the spectra for ALL1 and ALL3 samples, doublets 4, 5, and 6 (Fig. 1, Table II) were assigned to Fe^{3+} ions with contributions of 0.39 for ALL1 and 0.64 for ALL3. Doublets 4 and 5 represent trivalent iron in the more distorted M(3) site, whereas doublet no. 6 represents Fe^{3+} in the less distorted M(1) site. In the ALL2 spectrum Fe^{3+} is represented by two doublets nos. 4 and 6 where doublet no. 4 is assigned to the M(3) site and doublet no. 6 to the M(1) site. Figure 4a shows the relative contribution of Fe^{3+} ($\sum Fe^{3+} / \sum Fe$) vs. absorbed α-dose. As

can be seen in this figure the contribution of Fe^{3+} increases with α-dose. This is an unexpected result and can be explained in a similar way as the decrease in Fe^{2+} components with dose in Sect. 3.1. Figure 4b shows that the weighted averages of quadrupole splittings for Fe^{3+} components decrease with increasing absorbed α-dose.

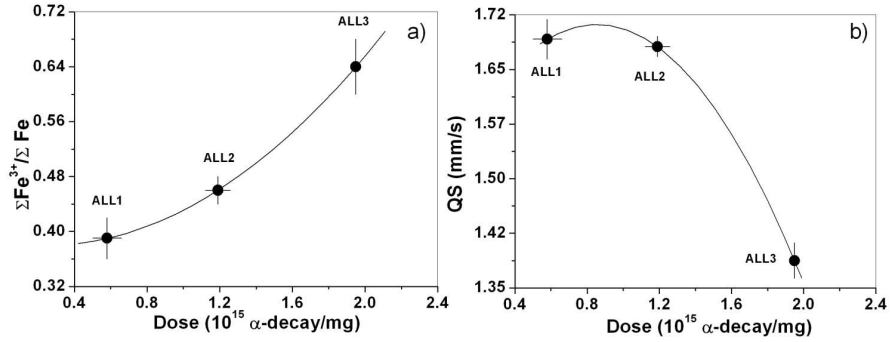

Fig. 4. (a) $\sum \mathrm{Fe}^{3+} / \sum \mathrm{Fe}$ vs. absorbed α-dose; the solid line represents polynomial fit: $\sum \mathrm{Fe}^{3+} / \sum \mathrm{Fe} = 0.384 - 0.042D + 0.089D^2$, correlation coefficient $r = 0.98$. (b) Average quadrupole splittings (QS) of Fe^{3+} components versus absorbed α-dose; the solid line represents polynomial fit: $\mathrm{QS} = 1.512 + 0.455D - 0.266D^2$, correlation coefficient $r = -0.91$.

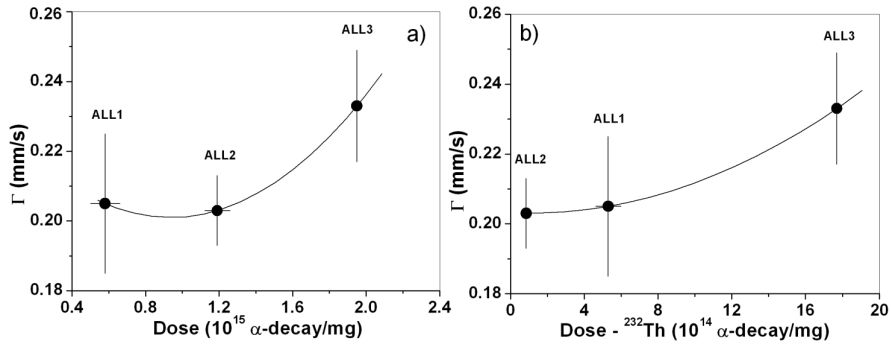

Fig. 5. Average line widths of Fe^{3+} components versus: (a) absorbed total α-dose and (b) absorbed α-dose from the ^{232}Th series. The solid lines represent polynomial regressions: $\Gamma = 0.228 - 0.058D + 0.031D^2$ and $\Gamma = 0.203 - 0.0002D_{\mathrm{Th}} + 0.0001D_{\mathrm{Th}}^2$. The correlation coefficients are $r = 0.87$ and 0.98, respectively.

The weighted averages of line widths of Fe^{3+} components vs. total α-dose and vs. α-dose from ^{232}Th are shown in Fig. 5. The plot demonstrates that better fitting is obtained when α-dose from ^{232}Th is taken instead of total α-dose. This relationship is very similar to that observed for quadrupole splittings of the Fe^{2+}

components. Thus, for partially metamict allanites the increase in line widths of Fe^{3+} doublets in the high degree is controlled by α-dose from ^{232}Th.

4. Conclusions

The divalent iron contribution in samples of allanite decreases with absorbed total α-dose. Weighted averages of the line widths of the Fe^{2+} and Fe^{3+} components slightly increase with absorbed α-dose. Weighted averages of quadrupole splitting values of the Fe^{2+} doublets increase with α-dose, whereas for Fe^{3+}, these values decrease. The increase in average quadrupole splittings for Fe^{2+} doublets and the average of line widths for Fe^{3+} doublets is better correlated with absorbed α-dose from ^{232}Th than total α-dose.

Acknowledgments

This work was supported by the State Committee for Scientific Research (Poland) through grant no. 2P04D06229.

References

[1] R.C. Ewing, *Nucl. Instrum. Methods Phys. Res. B* **91**, 22 (1994).

[2] W.J. Weber, R.C. Ewing, C.R.A. Catlow, T. Diaz de la Rubia, L.W. Hoobs, C. Kinoshita, H. Matzke, A.T. Motta, M. Nastas, E.K.H. Salje, E.R. Vance, S.J. Zinkle, *J. Mater. Res.* **13**, 1434 (1998).

[3] A. Meldrum, L.A. Boatner, W.J. Weber, R.C. Ewing, *Geochim. Cosmochim. Acta* **62**, 2509 (1998).

[4] D. Malczewski, J.E. Frąckowiak, E.V. Galuskin, *Hyperfine Interact.* **166**, 529 (2005).

[5] R.C. Ewing, R.F. Haaker, *Nucl. Chem. Waste Management* **1**, 51 (1980).

[6] W.A. Dollase, *Am. Mineral.* **56**, 447 (1971).

[7] A. Volborth, *Econ. Geol.* **57**, 209 (1962).

[8] D. Holtstam, *Geologiska Föreningens i Stockholm Förhandlinger* **126**, 149 (2004).

[9] R.A. Volkert, R.E. Zartman, P.B. Moore, *Precambrian Res.* **139**, 1 (2005).

[10] W.A. Dollase, *Z. Kristallogr.* **138**, 41 (1973).

[11] F.C. Hawthorne, L.A Groat, M. Raudsepp, N.A. Ball, M. Kimata, R. Gaba, N.M. Halden, G.R. Lumpkin, R.C. Ewing, R.B. Greegor, F.W. Lytle, T.S. Ercit, G.R. Rossman, F.J. Wicks, R.A. Ramik, B.L. Sherriff, M.E. Fleet, C. McCammon, *Am. Mineral.* **76**, 370 (1991).